

IMAGE DENOISING WITH UNION OF DIRECTIONAL ORTHONORMAL DWTS

Shogo MURAMATSU and Dandan HAN

Dept. of Electrical and Electronic Eng., Niigata University
8050 2-no-cho, Ikarashi, Nishi-ku, 950-2181, Niigata, Japan
E-mail: shogo@eng.niigata-u.ac.jp

ABSTRACT

A novel image denoising technique is proposed by using directional lapped orthogonal transforms (DirLOTs). DirLOTs satisfy orthogonality and the bases are allowed to be anisotropic with the fixed-critically-subsampling, overlapping, symmetric, real-valued and compact-support property. In this work, DirLOTs are used to construct directional symmetric orthonormal discrete wavelet transforms and then the bases are adopted to generate a redundant dictionary with several directions. The multiple directional property is suitable for representing natural images which contain diagonal edges and textures. The proposed dictionary is applied to solve the basis pursuit denoising problem. The denoising performance is evaluated for several images through the heuristic shrinkage and block-coordinate-relaxation algorithm. It is verified that the proposed technique is simple but yields perceptually preferable results.

Index Terms— DirLOT, Basis pursuit, Wavelet denoising, Heuristic shrinkage, Block-coordinate-relaxation algorithm

1. INTRODUCTION

In this study, we deal with a common problem of image denoising, i.e. removal of additive white Gaussian noise (AWGN) from a given image [1]. Let $\mathbf{x} \in \mathbb{R}^N$ be an observed image which is represented by

$$\mathbf{x} = \mathbf{x}^* + \mathbf{w},$$

where $\mathbf{x}^* \in \mathbb{R}^N$ and $\mathbf{w} \in \mathbb{R}^N$ are the original clean noiseless image and AWGN with zero mean and no correlation to the other pixels, respectively, i.e. $E\{\mathbf{w}\} = 0$ and $E\{\mathbf{w}\mathbf{w}^T\} = \sigma^2\mathbf{I}$.

Image denoising is a problem of finding a good candidate image $\hat{\mathbf{x}} \in \mathbb{R}^N$ of the unknown noiseless image \mathbf{x}^* only from the observed image \mathbf{x} . Popular denoising approaches include solvers for the basis pursuit denoising (BPDN) problem [1]. The BPDN problem assumes that the candidate $\hat{\mathbf{x}}$ is expressed by a linear-combination of image prototypes (atoms) in a dictionary $\mathbf{D} \in \mathbb{R}^{N \times L}$, i.e.

$$\hat{\mathbf{x}} = \mathbf{D}\hat{\mathbf{y}},$$

where $\hat{\mathbf{y}} \in \mathbb{R}^L$ is a candidate coefficient vector, and refers to the solution of the following form of optimization problem:

$$\hat{\mathbf{y}} = \arg \min_{\mathbf{y}} \frac{1}{2} \|\mathbf{x} - \mathbf{D}\mathbf{y}\|_2^2 + \lambda^T |\mathbf{y}|, \quad (1)$$

where $\|\cdot\|_2^2$ is the squared- ℓ_2 -norm of the argument, $\mathbf{y} \in \mathbb{R}^L$ is a coefficient vector and $\lambda \in \mathbb{R}^L$ is a parameter vector to control the trade-off between sparsity and reconstruction fidelity. If all elements

This work was supported by JSPS KAKENHI (23560443).

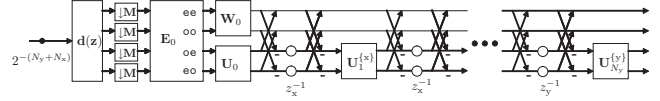


Fig. 1. Lattice structure of a DirLOT (forward transform)

of λ are the same as each other and represented by a scalar λ , the second term of the right hand side reduces to $\lambda \|\mathbf{y}\|_1$, where $\|\cdot\|_1$ is the ℓ_1 -norm of the argument.

There are several approaches to solve the BPDN problem in Eq. (1). The parallel-coordinate-descent (PCD) iterative-shrinkage is an example of such solvers, which is computationally efficient and applicable to large data such as images [1]. Furthermore, the PCD algorithm has a merit that it reduces to the block-coordinate-relaxation (BCR) algorithm when the dictionary \mathbf{D} is constructed as a union of unitary matrices and becomes more efficient [2]. A similar approach can also be found in the article [3]. The selection of the dictionary \mathbf{D} is a quite important task for building a BPDN solver since it influences not only the computational complexity but also the denoising quality.

Recent development of image transforms involves non-separable transforms for handling diagonal edges and textures since separable transforms are weak in representing such geometrical structures [4]. As a previous work, we have proposed 2-D non-separable directional lapped orthogonal transforms (DirLOTs) [5]. The bases are allowed to be anisotropic with the fixed-critically-subsampling, overlapping, orthogonal, symmetric, real-valued and compact-support property. The hierarchical tree construction yields a 2-D directional symmetric orthonormal discrete wavelet transform (DWT). A single DirLOT for a fixed direction, however, is less useful for natural images which contain rich amount of geometrical structures. There are two ways to overcome this drawback. One is local adaptive control of basis [6], and the other is redundant representation [1]. We adopt the latter case in this paper and consider adopting a union of tree-structured DirLOTs as a dictionary \mathbf{D} so that we can use the BCR algorithm for solving the BPDN problem.

2. REVIEW OF DIRECTIONAL LOTS

This section reviews DirLOTs and shows a design example.

2.1. Lattice Structure of 2-D Directional LOTS

DirLOTs can be constructed with a lattice structure as shown in Fig. 1 [5], where \mathbf{M} is a decimation matrix, $\mathbf{z} = (z_y, z_x)^T \in \mathbb{C}^2$ is a variable vector in the 2-D Z-transform domain and $\mathbf{d}(\mathbf{z})$ is a 2-D delay chain. The corresponding polyphase matrix of order $[N_y, N_x]^T$

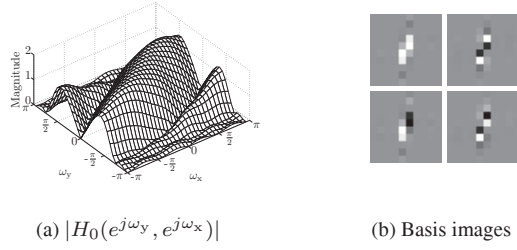


Fig. 2. A design example of DirLOT with the two-order TVMs of $\phi = \frac{\pi}{6}$ [rad], where $[N_y, N_x]^T = [4, 4]^T$, i.e. the basis size is 10×10 . Note that the vertical axis directs from top to bottom in (b).

is represented by the following product form:

$$\mathbf{E}(\mathbf{z}) = \prod_{n_y=1}^{N_y} \left\{ \mathbf{R}_{n_y}^{\{y\}} \mathbf{Q}(z_y) \right\} \cdot \prod_{n_x=1}^{N_x} \left\{ \mathbf{R}_{n_x}^{\{x\}} \mathbf{Q}(z_x) \right\} \cdot \mathbf{R}_0 \mathbf{E}_0, \quad (2)$$

where $\mathbf{Q}(z) = \frac{1}{2} \begin{pmatrix} \mathbf{I} & \mathbf{I} \\ \mathbf{I} & -\mathbf{I} \end{pmatrix} \begin{pmatrix} \mathbf{I} & \mathbf{O} \\ \mathbf{O} & z^{-1} \mathbf{I} \end{pmatrix} \begin{pmatrix} \mathbf{I} & \mathbf{I} \\ \mathbf{I} & -\mathbf{I} \end{pmatrix}$, $\mathbf{R}_0 = \begin{pmatrix} \mathbf{W}_0 & \mathbf{O} \\ \mathbf{O} & \mathbf{U}_0 \end{pmatrix}$, and $\mathbf{R}_n^{\{d\}} = \begin{pmatrix} \mathbf{I} & \mathbf{O} \\ \mathbf{O} & \mathbf{U}_n^{\{d\}} \end{pmatrix}$. The product of sequential matrices is defined by $\prod_{n=1}^N \mathbf{A}_n = \mathbf{A}_N \mathbf{A}_{N-1} \cdots \mathbf{A}_2 \mathbf{A}_1$. \mathbf{E}_0 is an $M \times M$ symmetric orthonormal transform matrix given directly through the 2-D separable discrete cosine transform (DCT), where M is the number of channels, i.e. $M = |\det \mathbf{M}|$. Symbols \mathbf{W}_0 , \mathbf{U}_0 and $\mathbf{U}_n^{\{d\}}$ denote orthonormal matrices of size $M/2 \times M/2$, which are freely controlled during the design process. The support region of each analysis (or synthesis) filter results in $2(N_y + 1) \times 2(N_x + 1)$.

Compared with existing transforms, DirLOTs have a special feature that the system has an ability to simultaneously satisfy the fixed-critically-subsampling, overlapping, orthonormal, symmetric, real-valued and compact-support property with a non-separable basis. As well, it can hold the trend vanishing moments (TVMs) for any direction [5]. The directional property works well for diagonal textures and edges.

2.2. Design Example

In the followings, the decimation matrix is set as $\mathbf{M} = \text{diag}(2, 2)$ in order to construct 2-D DWT trees. Figure 2 shows a design example of DirLOT of polyphase order $[N_y, N_x]^T = [4, 4]^T$. The design example was obtained through the genetic algorithm function “ga” of MATLAB R2011b, where the following accumulated error energy was used as the cost function:

$$\sum_{m=0}^3 \iint_{-\pi}^{\pi} \left\{ \left| R_m(e^{j\omega_y}, e^{j\omega_x}) \right| - \left| H_m(e^{j\omega_y}, e^{j\omega_x}) \right| \right\}^2 d\omega_y d\omega_x,$$

where $R_m(e^{j\omega_y}, e^{j\omega_x})$ and $H_m(e^{j\omega_y}, e^{j\omega_x})$ are the frequency responses of the m -th reference and analysis filter, respectively. For a given TVM direction $\phi \in [-\frac{\pi}{4}, \frac{3\pi}{4}]$, we define $R_0(e^{j\omega_y}, e^{j\omega_x})$ by

$$R_0(e^{j\omega_y}, e^{j\omega_x}) = \begin{cases} B(e^{j\omega_y}, e^{j\omega_x}), & \phi \in \{0, \frac{\pi}{2}\}, \\ B(e^{j\omega_y}, e^{j(\omega_x - \omega_y \cot \phi)}), & \phi \in [-\frac{\pi}{4}, 0) \cup (0, \frac{\pi}{4}], \\ B(e^{j(\omega_y - \omega_x \tan \phi)}, e^{j\omega_x}), & \phi \in [\frac{\pi}{4}, \frac{\pi}{2}) \cup (\frac{\pi}{2}, \frac{3\pi}{4}], \end{cases}$$

Data: Noisy image $\mathbf{x} \in \mathbb{R}^N$

Result: Denoised image $\hat{\mathbf{x}} \in \mathbb{R}^N$

Main process;

for $k \leftarrow 0$ to $K - 1$ do in parallel

$\mathbf{y}_k \leftarrow \frac{1}{K} \text{Shrink}(\Phi_k \mathbf{x});$

$\mathbf{u}_k \leftarrow \Phi_k^T \mathbf{y}_k;$

end

$\hat{\mathbf{x}} \leftarrow \sum_{k=0}^{K-1} \mathbf{u}_k;$

Algorithm 1: Heuristic shrinkage algorithm.

where $B(e^{j\omega_y}, e^{j\omega_x})$ is a 2-D maximally-flat frequency function $B(e^{j\omega_y}, e^{j\omega_x}) = 2A(e^{j\omega_y})A(e^{j\omega_x})$ defined through a 1-D maximally-flat frequency function

$$A(e^{j\omega}) = \left(\cos \frac{\omega}{2} \right)^{2P} \sum_{n=0}^{Q-1} d[n] \left(\sin \frac{\omega}{2} \right)^{2n},$$

where Q and P are the numbers of zeros at $\omega = 0$ and π , respectively, and the coefficients $d[n]$ are given by $d[n] = \frac{(P-1+n)!}{(P-1)!n!}$ [7]. References $R_m(e^{j\omega_y}, e^{j\omega_x})$ for $m = 1, 2, 3$ are specified by modulating $R_0(e^{j\omega_y}, e^{j\omega_x})$ to $(\omega_y, \omega_x)^T = (\pi, \pi)^T$, $(0, \pi)^T$ and $(\pi, 0)^T$, respectively.

Figure 2 shows a design example of $P = Q = 3$ and $\phi = \pi/6$ [rad], where $[N_y, N_x]^T = [4, 4]^T$. It is observed that the amplitude response of $H_0(e^{j\omega_y}, e^{j\omega_x})$ is flat along the direction $\mathbf{u}_\phi^T = (\sin \phi, \cos \phi)$ at $\omega^T = (\omega_y, \omega_x) = (0, 0)$.

3. DENOISING WITH UNION OF DIRLOTS

A single DirLOT has a drawback to represent multiple directional structures in images. In this section, we propose to construct a union of tree-structured DirLOTs as a dictionary \mathbf{D} and adopt the heuristic shrinkage and BCR algorithm for solving the BPDN problem [2].

3.1. Union of Directional Symmetric Orthonormal DWTs

A simple way to construct a redundant dictionary is to unite multiple unitary transforms. Shift invariant, i.e. non-subsampling, dictionary construction with orthonormal transforms is a popular example. The existing techniques, however, do not take account of the directional property. In this work, we propose to construct a dictionary by using multiple directional symmetric orthonormal wavelet transforms (DirSOWT) in order to sparsely represent diagonal textures and edges. Our proposed dictionary \mathbf{D} is represented by

$$\mathbf{D} = \left[\Phi_{0 \cup \frac{\pi}{2}}^T \quad \Phi_{\phi_1}^T \quad \Phi_{\phi_2}^T \quad \Phi_{\phi_3}^T \quad \cdots \quad \Phi_{\phi_{K-1}}^T \right], \quad (3)$$

where $\Phi_{0 \cup \frac{\pi}{2}}$ is a nondirectional symmetric orthonormal DWT with the classical two-order vanishing moments (VMs) [8], and Φ_ϕ is a DirSOWT constructed by a DirLOT with the two-order TVMs for the direction \mathbf{u}_ϕ [5]. K denotes the number of the DWTs, i.e. the redundancy of dictionary \mathbf{D} .

3.2. Heuristic Shrinkage (HS)

Since the set of atoms, i.e. column vectors, in \mathbf{D} is a normalized tight frame of \mathbb{R}^N and $\mathbf{D}\mathbf{D}^T = \sum_{k=0}^{K-1} \Phi_k^T \Phi_k = K\mathbf{I}$, we can apply the dictionary \mathbf{D} to the heuristic shrinkage. For the sake of

Data: Noisy image $\mathbf{x} \in \mathbb{R}^N$
Result: Denoised image $\hat{\mathbf{x}} \in \mathbb{R}^N$
Initialization;
 $i \leftarrow 0$;
 $\mathbf{y}^{(0)} \leftarrow \mathbf{0}$;
 $\hat{\mathbf{x}}^{(0)} \leftarrow \mathbf{D}\mathbf{y}^{(0)} = \sum_{k=0}^{K-1} \Phi_k^T \mathbf{y}_k^{(0)} = \mathbf{0}$;
 $\mathbf{r}^{(0)} \leftarrow \mathbf{x} - \hat{\mathbf{x}}^{(0)} = \mathbf{x}$;
Main iteration to find $\mathbf{y}^T = (\mathbf{y}_0^T, \mathbf{y}_1^T, \dots, \mathbf{y}_{K-1}^T)$ that minimizes $f(\mathbf{y}) = \frac{1}{2} \|\mathbf{x} - \mathbf{D}\mathbf{y}\|_2^2 + \lambda^T |\mathbf{y}|$;
repeat
 $i \leftarrow i + 1$;
 $\mathbf{u} \leftarrow \hat{\mathbf{x}}^{(i-1)}$;
 $\mathbf{z} \leftarrow \mathbf{r}^{(i-1)}$;
 for $k \leftarrow 0$ to $K - 1$ do
 $\mathbf{y}_k^{(i)} \leftarrow \text{Shrink}(\mathbf{y}_k^{(i-1)} + \Phi_k \mathbf{z})$;
 $\mathbf{u} \leftarrow \mathbf{u} + \Phi_k^T (\mathbf{y}_k^{(i)} - \mathbf{y}_k^{(i-1)})$;
 $\mathbf{z} \leftarrow \mathbf{x} - \mathbf{u}$;
 end
 $\hat{\mathbf{x}}^{(i)} \leftarrow \mathbf{u}$;
 $\mathbf{r}^{(i)} \leftarrow \mathbf{z}$;
until $\|\mathbf{y}^{(i)} - \mathbf{y}^{(i-1)}\|_2 / \|\mathbf{y}^{(i)}\|_2 < \epsilon$;
 $\hat{\mathbf{x}} \leftarrow \hat{\mathbf{x}}^{(i)}$;

Algorithm 2: BCR iterative-shrinkage algorithm.

simplification, let us denote $\Phi_0 = \Phi_{0 \cup \frac{\pi}{2}}$ and $\Phi_k = \Phi_{\phi_k}$ for $k = 1, 2, \dots, K - 1$, respectively. Then, the heuristic shrinkage for \mathbf{D} is written as shown in Algorithm 1 [1], where $\mathbf{y}_k \in \mathbb{R}^N$ is the k -th subvector of $\mathbf{y} \in \mathbb{R}^{KN}$, and $\text{Shrink}()$ is the vector function that performs the scalar soft-shrinkage operation

$$\hat{\mathbf{y}} = \text{Shrink}(\mathbf{y}) = \text{sign}(\mathbf{y}) \cdot (|\mathbf{y}| - \lambda)_+,$$

where $(\cdot)_+$ replaces negative elements to zeros and remains positive elements. The heuristic shrinkage corresponds to the first iteration of the PCD algorithm for solving the BPDN problem in Eq. (1) and gives appropriate denoising results with simple computation [1]. Notice that Algorithm 1 only takes the average of the results of independent orthonormal wavelet shrinkage operations.

3.3. BCR Iterative-Shrinkage

The previous heuristic shrinkage approach has a drawback that fine details are averaged out. This fact is readily understood since a multiple-DWT dictionary contains multiple scaling filters and the responsible coefficients of details are diluted out. In order to solve this dilution problem, we can exploit the redundancy of \mathbf{D} and more sophisticated algorithms can be used for sparser representation [1].

Since our dictionary is a union of unitary matrices, the BCR algorithm is available. Algorithm 2 shows the procedure. The BCR algorithm iteratively updates the solution of the following subproblem:

$$\begin{aligned} \hat{\mathbf{y}}_k &= \arg \min_{\mathbf{y}_k} \frac{1}{2} \left\| \mathbf{x} - \tilde{\mathbf{x}} - \Phi_k^T (\mathbf{y}_k - \tilde{\mathbf{y}}_k) \right\|_2^2 + \lambda_k^T |\mathbf{y}_k| \\ &= \arg \min_{\mathbf{y}_k} \frac{1}{2} \left\| (\tilde{\mathbf{y}}_k + \Phi_k \tilde{\mathbf{r}}) - \mathbf{y}_k \right\|_2^2 + \lambda_k^T |\mathbf{y}_k| \end{aligned}$$

and converges to a solution of Eq. (1), where $\tilde{\mathbf{x}}$, $\tilde{\mathbf{y}}_k$ and $\tilde{\mathbf{r}}$ are the estimations of $\hat{\mathbf{x}}$, \mathbf{y}_k and \mathbf{r} in the previous step, respectively, and $\lambda_k \in \mathbb{R}^N$ is the k -th subvector of λ , i.e. $\lambda^T = (\lambda_0^T, \lambda_1^T, \dots, \lambda_{K-1}^T)$.

Table 1. Adopted transforms and the features.

Abrv.	Features
DB5	Daubechies' least asymmetric compactly-supported wavelet with five VMs, separable, orthonormal
SON4	Symmetric orthonormal DWT with two VMs of $[N_y, N_x]^T = [4, 4]^T$, nonseparable, nondirectional
NSCT	Nonsampled contourlet with $2^3, 2^3, 2^4, 2^4$ directions in the scales from coarser to finer, near tight, symmetric [9]
UDN4	Union of SON4 and DirSOWTs with two TVMs of $[N_y, N_x]^T = [4, 4]^T$, multidirectional, tight, symmetric

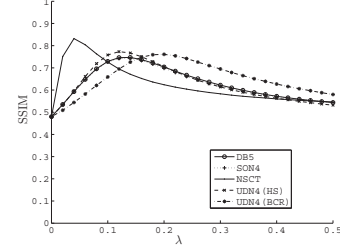


Fig. 3. Denoising evaluation in terms of SSIM index for “barbara” with AWGN ($\sigma = 20$).

4. EXPERIMENTAL RESULTS

This section shows some experimental results of shrinkage image denoising, and verifies the significance of our proposed dictionary \mathbf{D} in Eq. (3). To assess the performance, it is compared with some other transforms. The transforms adopted in this experiments are summarized in Tab. 1, where UDN4 denotes the proposed dictionary \mathbf{D} consisting of multiple DirSOWTs of $[N_y, N_x]^T = [4, 4]^T$. We select 18 angles for ϕ_k in Eq. (3) as $\phi_k \in \{-\frac{4\pi}{18}, -\frac{3\pi}{18}, -\frac{2\pi}{18}, \dots, \frac{13\pi}{18}\}$. Thus, the redundancy results in $K = 1 + 18 = 19$.

For comparison, we also show the denoising performances through the Daubechies' least asymmetric compactly-supported orthonormal wavelet with the five-order VMs (DB5) and single symmetric orthonormal wavelet $\Phi_0 = \Phi_{0 \cup \frac{\pi}{2}}$ of $[N_y, N_x]^T = [4, 4]^T$ (SON4), where every filter is of size 10×10 . The number of levels of each DWT is set to seven. For a reference of redundant dictionary, we also show the performance of nonsampled contourlet transform (NSCT) [9]. We adopt the four-scale construction with $2^3, 2^3, 2^4, 2^4$ directions in the scales from coarser to finer, where the design examples in [9, Sec.III-D] are used¹. The redundancy is $1 + 2^3 + 2^3 + 2^4 + 2^4 = 49$.

The task of determining the parameter λ is not trivial. In the followings, we first evaluate the proposed denoising by setting λ in the form $\lambda \mathbf{1}_w$ and sweeping the scalar parameter λ , where $\mathbf{1}_w \in \mathbb{R}^N$ is the vector of which elements at scaling and wavelet coefficient positions are zeros and ones, respectively. Then, we consider applying BayesShrink to adaptively determine the threshold values, i.e. parameter λ [10].

4.1. Denoising Results with Scalar Parameter λ

The eight-bit grayscale image of size 512×512 “barbara” was used as a test image, where the noise level is $\sigma = 20$ and the intensity is normalized to $[0, 1]$ during the denoising process.

¹NSCT toolbox from MATLAB Central (<http://www.mathworks.com/matlabcentral/>) was used.

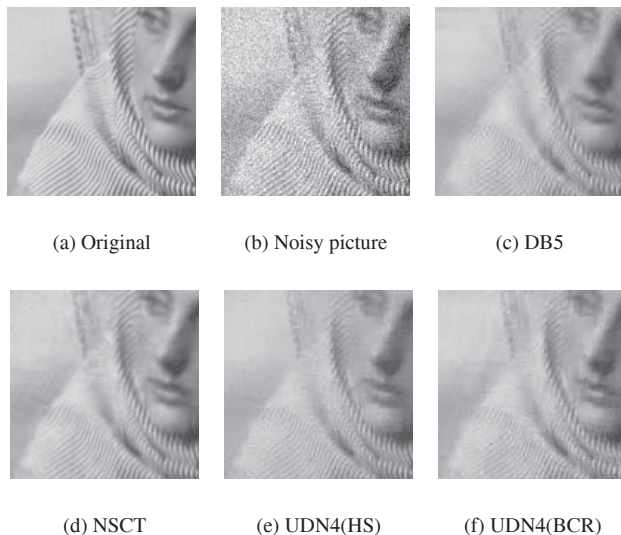


Fig. 4. Denoising results. (a)Original picture, (b) Noisy picture with AWGN ($\sigma = 20$), (c)-(f) Denoised pictures.

Table 2. Comparison of SSIM indexes among four transforms for various pictures and noise levels, where BayesShrink was used to determine the parameter λ for every case.

	σ	DB5	SON4	NSCT (HS)	UDN4	
					(HS)	(BCR)
goldhill	20	0.726	0.723	0.753	0.746	0.725
	30	0.668	0.664	0.666	0.684	0.664
	40	0.625	0.621	0.592	0.640	0.621
lena	20	0.794	0.793	0.780	0.814	0.792
	30	0.749	0.748	0.693	0.768	0.748
	40	0.719	0.720	0.616	0.736	0.720
barbara	20	0.748	0.760	0.767	0.778	0.750
	30	0.680	0.671	0.687	0.681	0.685
	40	0.626	0.608	0.619	0.623	0.633
baboon	20	0.668	0.714	0.757	0.698	0.730
	30	0.558	0.606	0.653	0.591	0.613
	40	0.486	0.515	0.566	0.505	0.523

Figure 3 shows a variation of structural similarity (SSIM) indexes against the value of λ . For NSCT, we compensated the threshold λ by using the weight $1/32, 1/8, 1/4$ and 1 for the scales from coarser to finer. The SSIM index is a similarity measure of two images, which approaches to one when the two images are perceptually close to each other² [11]. From Fig. 3, it is observed that NSCT scores the highest quality in terms of SSIM around at $\lambda = 0.05$. On the other hand, UDN4 is less sensitive to the choice of λ and gives appropriate performance with both of the HS and BCR approaches. Figures 4 subjectively compares the denoising performances among three transforms for “barbara” by using the optimum λ in Fig. 3.

4.2. Denoising Results with BayesShrink

The eight-bit grayscale images of size 512×512 “goldhill,” “lena,” “barbara” and “baboon” are used as test images with different

²MATLAB function `ssim_index.m` from <http://www.cns.nyu.edu/~lcv/ssim/> was used.

noise levels $\sigma = 20, 30, 40$. Table 2 compares the denoising performance with BayesShrink among four transforms in Tab. 1 [10], where the robust median estimator was applied to the finest wavelet coefficients for estimating the noise variance. Every value was obtained by averaging the results of five trials. For NSCT, we compensated the estimated variance by using the weight $1/32, 1/8, 1/4$ and 1 for the scales from coarser to finer. From the table, it is observed that UDN4 with the heuristic shrinkage shows almost the best performance for “goldhill” and “lena” among the four transforms. Although NSCT performs better than UDN4 for “barbara” and “baboon”, which contain fine textures, the BCR-approach slightly improves the performance of UDN4 and shows the prospective performance of other iterative-shrinkage approaches.

5. CONCLUSIONS

A novel image denoising technique was proposed by using DirLOTs. We constructed directional symmetric orthonormal DWTs and adopted the bases to generate a redundant multi-directional dictionary. Through the application to the BPDN solver, it is verified that the proposed dictionary yields perceptually preferable results with a simple computation.

6. REFERENCES

- [1] M. Elad, “Why simple shrinkage is still relevant for redundant representations?,” *IEEE Trans. Inf. Theory*, vol. 52, no. 12, pp. 5559–5569, Dec. 2006.
- [2] S. Sardy, A. G. Bruce, and P. Tseng, “Block coordinate relaxation methods for nonparametric wavelet denoising,” *J. Comput. Graphical Statist.*, vol. 9, pp. 361–379, 2000.
- [3] P. Ishwar, K. Ratakonda, P. Moulin, and N. Ahuja, “Image denoising using multiple compaction domains,” in *IEEE Proc. of ICASSP*, May 1998, vol. 3, pp. 1889–1892.
- [4] J.-L. Starck, F. Murtagh, and J. M. Fadili, *Sparse Image and Signal Processing: Wavelets, Curvelets, Morphological Diversity*, Cambridge University Press, 2010.
- [5] S. Muramatsu, T. Kobayashi, D. Han, and H. Kikuchi, “Design method of directional GenLOT with trend vanishing moments,” in *Proc. of APSIPA ASC*, Dec. 2010, pp. 692–701.
- [6] S. Muramatsu and M. Hiki, “Block-wise implementation of directional GenLOT,” in *IEEE Proc. of ICIP*, Nov. 2009, pp. 3977–3980.
- [7] P. P. Vaidyanathan, “On maximally-flat linear-phase FIR filters,” *IEEE Trans. Circuits Syst.*, vol. 31, no. 9, pp. 830–832, Sept. 1984.
- [8] T. Kobayashi, S. Muramatsu, and H. Kikuchi, “Two-degree vanishing moments on 2-D non-separable GenLOT,” in *IEEE Proc. of ISPACS*, Dec. 2009, pp. 248–251.
- [9] A. L. da Cunha, J. Zhou, and M. N. Do, “The nonsubsampling contourlet transform: Theory, design and applications,” *IEEE Trans. Image Process.*, vol. 15, no. 10, Oct. 2006.
- [10] S. G. Chang, B. Yu, and M. Vetterli, “Adaptive wavelet thresholding for image denoising and compression,” *IEEE Trans. Image Process.*, vol. 9, no. 9, pp. 1532–1546, Sept. 2000.
- [11] Z. Wang, A. C. Bovik, H. R. Sheikh, and E. P. Simoncelli, “Image quality assessment: From error visibility to structural similarity,” *IEEE Trans. Image Process.*, vol. 13, no. 4, pp. 600–612, Apr. 2004.